



Research solution for automatic hole quality analysis when drilling fiber-reinforced composites

Andrii Hrechuk¹ · Mikael Hörndahl¹ · Fredrik Schultheiss¹

Received: 13 March 2023 / Accepted: 31 May 2023 / Published online: 13 June 2023
© The Author(s) 2023

Abstract

Fiber-reinforced polymers are highly demanding composites in aerospace and automotive areas because of their excellent mechanical properties such as stiffness and strength-to-weight ratio. The drilling remains the major machining operation applied to composites to provide high-quality holes for joints between parts. Due to composites plied structure, the drilling is accompanied with unusual form metal cutting defects such as delamination and uncut fibers around the drilled hole. Considering that the tool life of some drills reaches over thousands of holes, the research of composites machinability becomes difficult due to demanded labor intensity in manual inspection of the hole quality. Therefore, this paper develops the research solution for automatic analysis of the hole quality in drilled fiber-reinforced materials. The paper proposes a complex of solutions aimed to speed up the analysis of the hole quality when composites drilling. The solution consists of the developed vacuum table, robot arm with high-speed camera, developed top and bottom lightning systems, and Image Processing algorithms for defect detection from captured images. The paper results show how the developed solution can be used for high routine research activities. The output data, including tested 72 cutting data parameters and full-size tool life test, allowed identifying the operational window for high-speed steel drills and the range of tool life, where drill ensures a certain hole quality. The paper shows the efficiency of the developed research solution can reach 5 s per hole including drilling and full cycle of measurements having measurement error of 1–3%.

Keywords Hole quality · Automation · Image processing · Biocomposites · Drilling

1 Introduction

Fiber-reinforced polymers (FRP) were introduced in the 1950s as an alternative to metal-based materials, which tended to corrode [1, 2]. The advantage of these FRP includes high strength-to-weight and stiffness-to-weight ratios, a low coefficient of thermal expansion, and magnetic and corrosion resistance [1, 2]. Additionally, complex parts are possible to be directly produced in these materials with near-net shape and high tolerances. All these properties and features make composite materials demanding in aerospace and other industries.

FRP material products are commonly designed to minimize machining operations; however, these operations are often essential to provide reliable mechanical joints

between parts. For instance, in the aeronautical industry, assembly of the overall airframe may take 50% of the total fabrication time and account for more than 20% of the total production cost [3]. Thus, a remaining task in the production of FRP is hole-making operations, e.g., drilling, for instance provide reliable joining or other accurate geometries otherwise difficult to produce. Drilling of FRP is accompanied by a whole range of unique defects, special to the material type, which does not occur during drilling metallic materials. For instance, these defects include uncut fibers, delamination, surface damage, and thermal decomposition. Overall, FRP materials have a poor machinability due to their inhomogeneity, anisotropy, and the presence of hard and abrasive fibers [4, 5]. FRP materials, comprising adjoining fiber layers, are more sensitive to drilling forces when compared to metallic materials [6]. For instance, high and concentrated forces may result in delamination of the FRP material [7–9]. When drilling FRP materials, the axial thrust may result in delamination and interlayer cracking on the exit side where

✉ Andrii Hrechuk
andrii.hrechuk@iprod.lth.se

¹ Lund University, Ole Römers väg 1, SE-221 00 Lund, Sweden

a low laminate thickness at the end of machining provides a lower resistance for tool penetration [10]. These defects may for instance have a negative effect on the reliability of bolted and riveted connections as they inherently create gaps in the joint due to bending of uncut fibers, as opposed to parts without defects which fit tightly together. These gaps lead to loose joints which in many applications is unacceptable due to strength and reliability reasons. Therefore, the quantitative evaluation of drilled hole defects in FRP components is an important task to increase the efficiency of the assembly process and to optimize the drilling process parameters, with the aim of increasing the performance and reliability of the product.

In addition to the common parameters cylindricity, waviness, roughness, and axial straightness, delamination, burr formation, spalling, chipping, and fuzzing are all important parameters specific to the drilling of FRP. A complicating factor is also uncertainties on the material properties of the laminate itself, which can be affected by residual porosity from the material production phase. Thus, the complex nature of defect formation in FRP materials commonly implies the need for studying each hole under a light-optical microscope to gauge the quality of the hole. Many different methods have been presented for the analysis of damage types in drilling FRP materials.

These techniques include radiographic Image Processing [11], C-scan [12], CT scan and SEM [13], surface profilometry [14], and stereoscopic microscopy [15]. However, the time and effort required for this type of inspection on the large number of holes usually drilled in FRP often inhibit any large-scale inspection or trial protocol purely due to practical reasons. This is because large datasets comprising of several thousands of holes are required to gain a better understanding of the defect formation and tool wear mechanisms when drilling FRP.

Thus, this paper develops and demonstrates our vision and respective systemic solution to accelerate the research of composite drilling. It is aimed to create the research solution which aims to provide the drilling setup, fast and accurate scanning of the drilled holes, and a set of hardware and software features which allows analyzing the drilled holes. The following section explains the developed solution which consists of vacuum table for drilling, robotic arm with high-speed camera, and decision-making system. The solution is exemplified on the biocomposite drilling using HSS drills.

2 Developed solution for research on drilling

To satisfy the formulated goals, the proposed research solution for automated analysis of drilling FRP consists of vacuum table, measurement station, and decision-making protocol and respective algorithms—see Fig. 1. Vacuum table is designed for drilling significant number of holes in FRP panel, measurement station provides automatic capturing drilled holes following the predefined pattern of hole positions, and decision-making unit or block is an algorithmic solution which provides the quantification of the images of the captured holes and hole defects.

2.1 Vacuum table

The first part of the proposed solution is vacuum table for enabling drilling of FRP panels. The vacuum table displayed in Fig. 1 and Fig. 2a is designed for drilling FRP panels for the research purposes. The design solves the following tasks: drilling without backside support, fast chip and dust

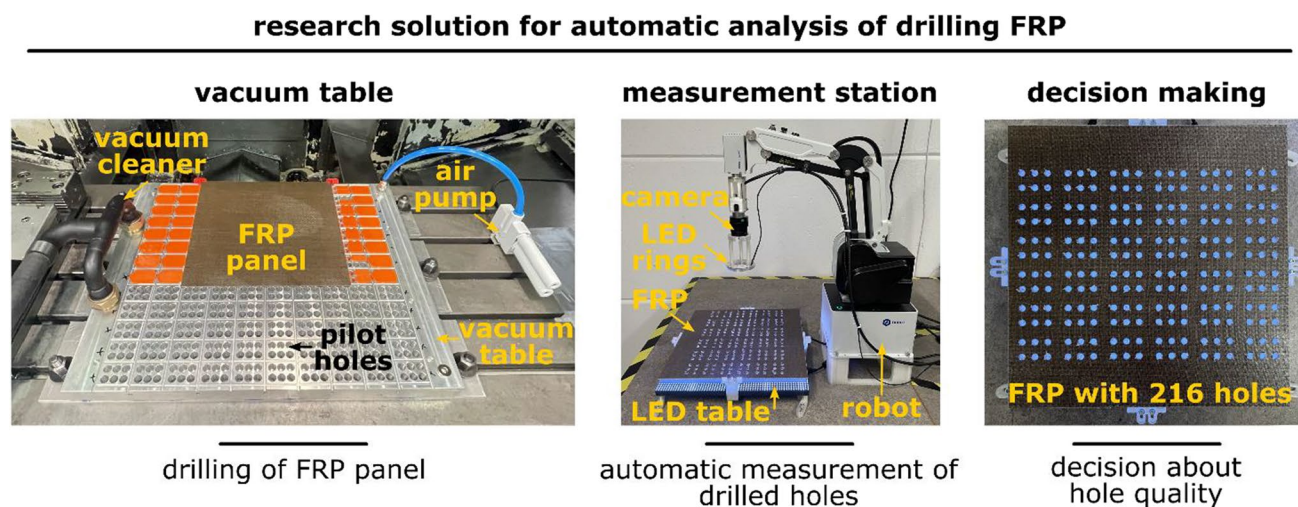


Fig. 1 The design of the research solution for automatic analysis of drilling FRP panel

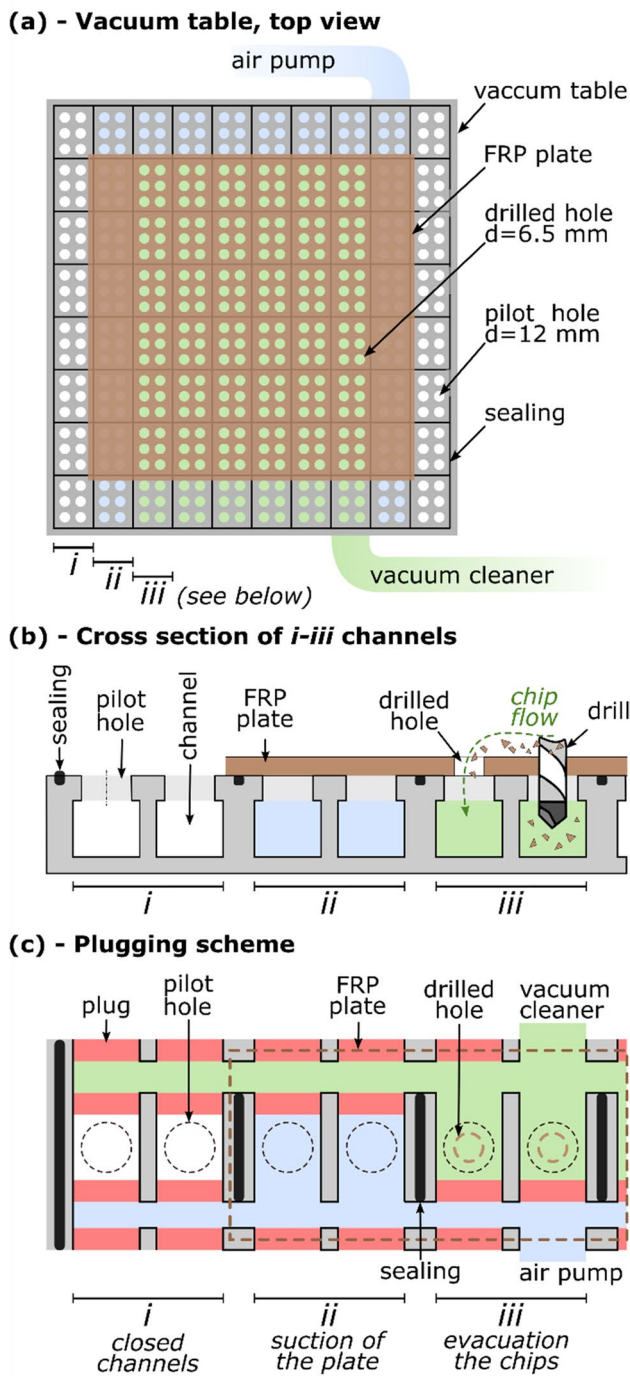


Fig. 2 The design of vacuum table. **a** The vacuum table has pilot holes, sealing channels, and air channels. The design allows changing connection configuration depending on the size of FRP panel needed to be drilled. **b** When the channels configured for specific panel, some channels are closed, and other is used for suction of the panel to the table and other for safe evacuation of the chips. **c** Independently from the panel size, the plugging scheme includes connected air pump from one side and vacuum cleaner from another

evacuation, simple clamping of the panel, and being adaptable for different panel size.

When drilling with backside support such as aluminum, FRP defects such as delamination and uncut fibers can be avoided entirely in the hole exit [16]. However, many automotive and aerospace applications require drilling without backside support due to the lack of space around parts, the curved shape of parts, and others. Thus, the FRP machinability investigation, including the defect analysis, needs to be done in similar conditions. The pilot holes with a diameter of 12 mm and a depth of 22 mm provide sufficient space underneath the panel enabling drilling without support. At the same time, the 12-mm pilot hole supports the drilling region preventing its bending. Because the delamination size usually does not exceed 2 mm in the radial direction around the hole edge, the selected size of the drilled holes enables the use of drills up to 10 mm in diameter.

The channels inside the vacuum table and the sealing enforce the chip and dust evacuation and panel clamping. Channels are milled along the vacuum table connecting pilot holes row by row (Fig. 2b). On the table ends, channels are connected. The plugging system (shown in Fig. 2c) closes channels into two contours. The first closed contour clamps the panel to the table by suction of the air using a connected air pump. The second contour provides the chip evacuation from the drilled holes. The sealing between the plate and the table prevents pressure leakage.

The proposed chip removal method can be compared to “external-rotation internal-chip removal tool handle” proposed by Xu et al. [17] and “suction-type internal chip removal drilling system” proposed by Wang et al. [18] used in composite drilling. Both chip removal handles are placed on the tool spindle collecting the chip via the pipe to the chip collector. Such methods rely on collecting the chip from the top, while the vacuum table sucks the chip from below. Both methods can be considered reliable for chip collection; however, they provide different capabilities. The tool handle is handy on small milling machines with limited space and without enclosure. Since the chip rises, the tool handle is very efficient in capturing the chip. The vacuum table is more versatile since it does not require any attachment to the drilling spindle. Therefore, attachments such as a rotational force-torque sensor or transducer for ultrasonic drilling can be installed. The vacuum table collects the chip through the pilot holes that create a larger surface for chip collecting for the chip which settles down.

Since the thrust force is driven downwards when drilling, the used suction pressure in the axial direction is sufficient for clamping during the machining. No macro- or micro-shifting of the plate has been noticed during tests. Chip evacuation occurs in two ways. First, the chip is suctioned through the neighboring drilled holes and secondly through the channel underneath the pilot hole—see Fig. 2c.

The designed vacuum table has 780 pilot holes and can fit the plate of 500 × 500 mm. Two rows of pilot holes always

must be used for the suction clamping; thus, maximum of 660 holes can be drilled using the table. The example of clamping 300×300 mm plate with 216 drilled holes is shown in Fig. 1 and Fig. 2a.

The proposed design of the vacuum table is a reliable solution for carrying out drilling tests on any CNC mill—however, the setup was not tested for vibration-assisted drilling. The practical importance is that the developed vacuum table provides the following: high efficiency in the drilling of large variety of the composite panels of different size, fast clamping and releasing of the drilled panels, in-process chip evacuation, and drilling without backside support.

2.2 Measurement station

The scanning of holes is the next step when the FRP panel is already drilled. We propose a measurement station consisting of a robot arm, camera, and lighting system for automatizing the scanning process. The idea is to capture the drilled holes in the same sequence as it was drilled. The robot provides movement of the camera parallel to the mounted panel.

The used robot is Dobot MG400 with a payload of 500 g, 4° of freedom, 0.02-mm positioning precision, and 0.01 mm of repeatability—see Fig. 1. The maximum movement speed of the joint is 300°/s. The reachability of the robot is 320 mm from the robot base, which is sufficient for a FRP plate of 300×300 mm.

The camera is mounted on the robot arm. The camera holder is custom designed and 3D printed. The selected Basler acA1440-220uc RGB camera module is used with Computar M3Z1228C-MP varifocal lens. This combination provides the resolution of 1080×1080 pixels for the region of 22×22 mm of actual size. Therefore, each pixel of the images corresponds to $20 \mu\text{m}$ of the actual object dimensions. It gives sufficient resolution for defect detection in a rational memory usage and frame rate of 227 fps. The maximum camera exposition of 50,000 s provides sufficient light balance, but the complex morphology of defects requires an additional light source. The working distance of the camera is 100 mm, and it allows for installation of an additional lighting between the camera and the drilled panel.

A. Maghami et al. [19] proposed to use four directed light to highlight drilling-induced defects in CFRP by image fusion. It allowed to obtain better visibility of defects comparing to conventional dark-field lighting. In our case, we propose to use intensive and color light underneath the drilled hole and two levels of focused light from to the top.

Light solution includes two individual light rings mounted on the camera; see Fig. 3. Rings are mounted into the custom-made holder, which does not block the camera view. The small inner ring has 16 RGB LEDs, and the outer ring has 24 RGB

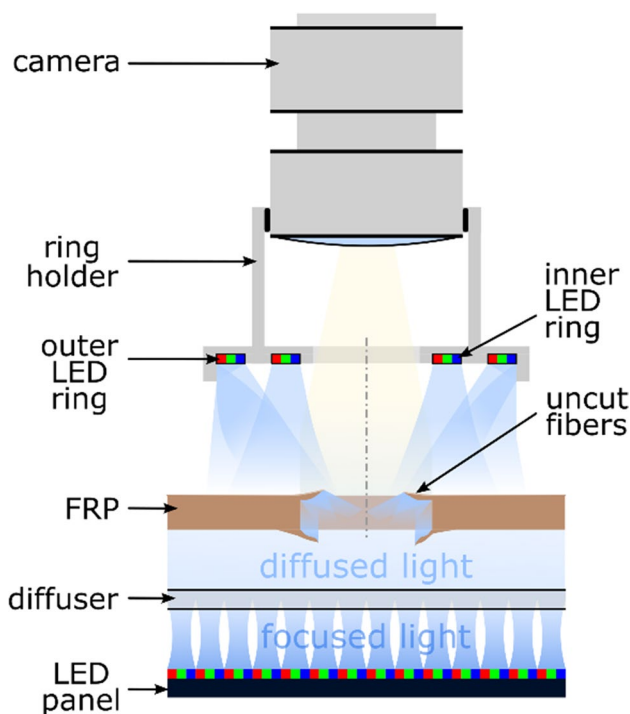


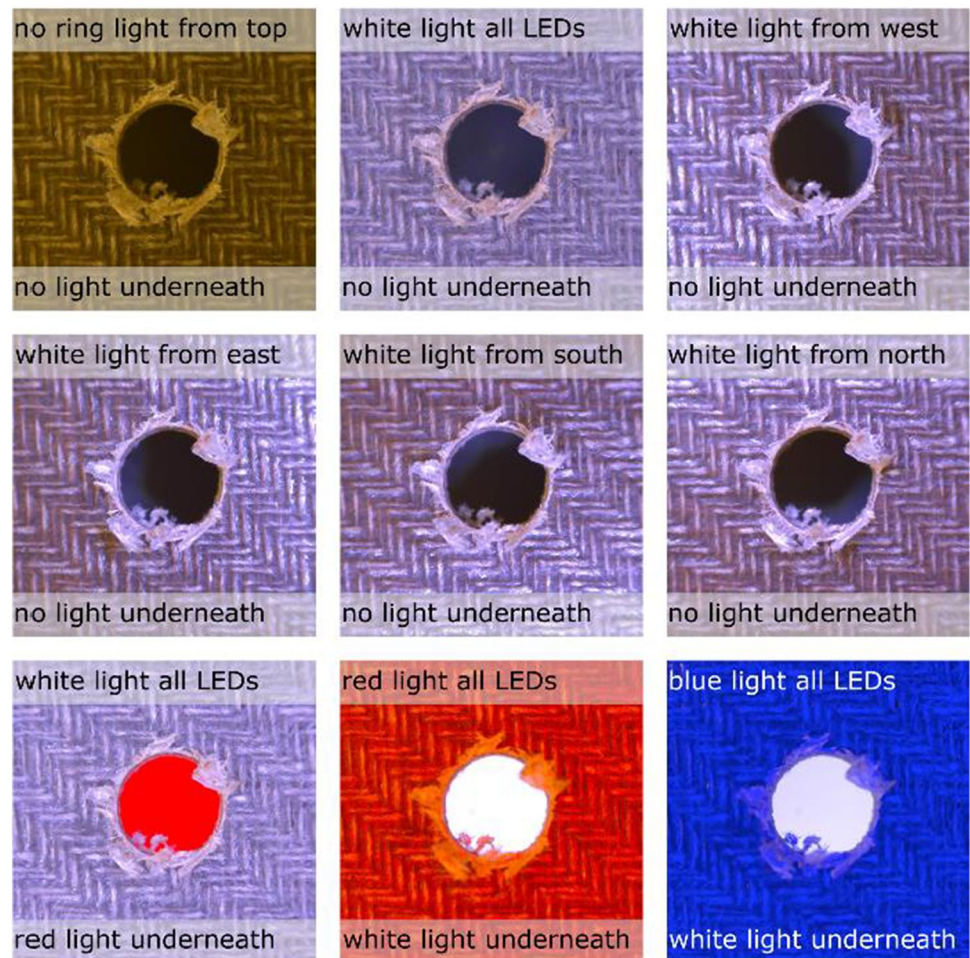
Fig. 3 The lighting system. Two separate LED rings provide an additional light source from the top, and the LED panel with diffuser changes the background color

LEDs controlled by the WS2812 driver. Ring internal sizes are 52.3 mm and 31.7 mm, respectively. Thus, the inner ring is closer to the drilled hole, providing more focused light, while the outer ring gives more spread light around the drilled hole. The combination of these rings allows focusing the defects and (or) creating the shadows to highlight needed defects.

The background color is not less important for defect highlighting. Brighter FRPs (e.g., GFRP) need a darker background to keep defects visible, and darker FRPs (e.g., CFRP) need brighter background. To enable a change in the background color, the light table was developed. This solution includes a panel with 4096 RGB LEDs and a black acrylic diffuser underneath the FRP panel. LED panel provides direct light, which diffuses through an acrylic plate. It gives the smooth and uniform lighting of the FRP panel. Since the diffuser is initially black, the background is black by default.

Both rings and the LED panel are controlled by PC using Python. It allows changing the color and light intensity of an individual LED element. Addressing certain LEDs, the developed lighting system combines top and background light highlighting specific defects. The method novelty is a combination of the top and bottom light creating the various combinations of the light which are shown in Fig. 4—demonstrated on the drilled hole in Flax/PLA biocomposite. There are changes in light direction and color for the ring LEDs and background color

Fig. 4 Combinations of different light colors and directions of ring LEDs and the background color from the LED panel underneath the FRP plate



from black to white. It is seen that different combinations highlight hole defects around and inside the hole.

The partial importance of the developed light system corresponds to versatility of the set bright/contrast conditions to improve defect visibility. The brighter composites such as glass fiber or natural fiber composites may need darker background to provide sufficient contrast between uncut fibers and the background color. Darker composites such as carbon fiber may need brighter backgrounds. The combination of the contrast colors such as red on top LEDs and white on bottom LEDs allows for avoiding natural artifacts such as reflections or dust on the top surface. Applying the high intensity to the top LEDs, the natural color of the composite can be enhanced or neglected to create better light/contrast conditions for defect detection. Such contrast enhancement simplifies the Image Processing stage, increases measurement accuracy, and, in some cases, enables measurements.

2.3 Decision-making unit

The images of captured holes should be analyzed and quantified for further decision-making. Since the robotic arm follows the predefined pattern capturing each drilled hole changing the light, the measurement system fills the database of the drilled holes. Here, the Image Processing techniques are implemented to detect hole defects. Various light combinations allow simplifying Image Processing procedures by adjusting the brightness and contrast conditions for particular FRP type, ambient light, and other.

The hole contours with defects are measured using certain metrics. Metrics or criteria such as delamination factors F_d [6] and F_a [20], uncut fiber area [21], and new topological metric impenarity [22, 23] are widely used for defect quantification. Calculated metrics complements the created database of images. Finally, the database is analyzed using the clustering or the threshold for used metric.

3 Methods

The developed research solution represents the chain from the drilling operation of FRP to scanning, measuring, and analyzing the drilled hole in the fastest way. Current section shows how the developed solution can be used for investigation of the FRP machinability as exemplified by drilling Flax/PLA biocomposite using HSS drills.

3.1 Setup, tools, and composites

Flax/PLA biocomposite with 60/40 fiber/matrix ratio, twill 4/4 woven scheme, and 2 mm of thickness was used to demonstrate the operation of the developed solution. Biocomposites have been produced by Flaxco, Belgium.

Preliminary tests done by Hindupur [24] showed that cutting edge radius plays the crucial role in biocomposite drilling. Furthermore, HSS drills showed the highest hole quality compared to PCD, uncoated and CVD diamond coated drills. Therefore, the standard HSS twist drills with diameter of 6.5 mm were used for the drilling operation. The diameter was taken to expand the cutting speed range—based on the maximum of 12,500 RPM in used milling machine. The measured cutting edge radius CER was 8 μm on average along the main cutting edges. The wedge angle on the periphery was 45°. Tool geometry was measured using Alicona InfiniteFocus 3D.

The drilling was carried out on a CNC milling machine Bridgeport CX1540 with a maximum of 12,500 RPM. The developed vacuum table has been installed in the milling machine (see Fig. 1a). Because of the panel size of 300 \times 300 mm and the predefined pattern of the pilot holes in the table, 216 holes were drilled per plate according to the scheme in Fig. 2a.

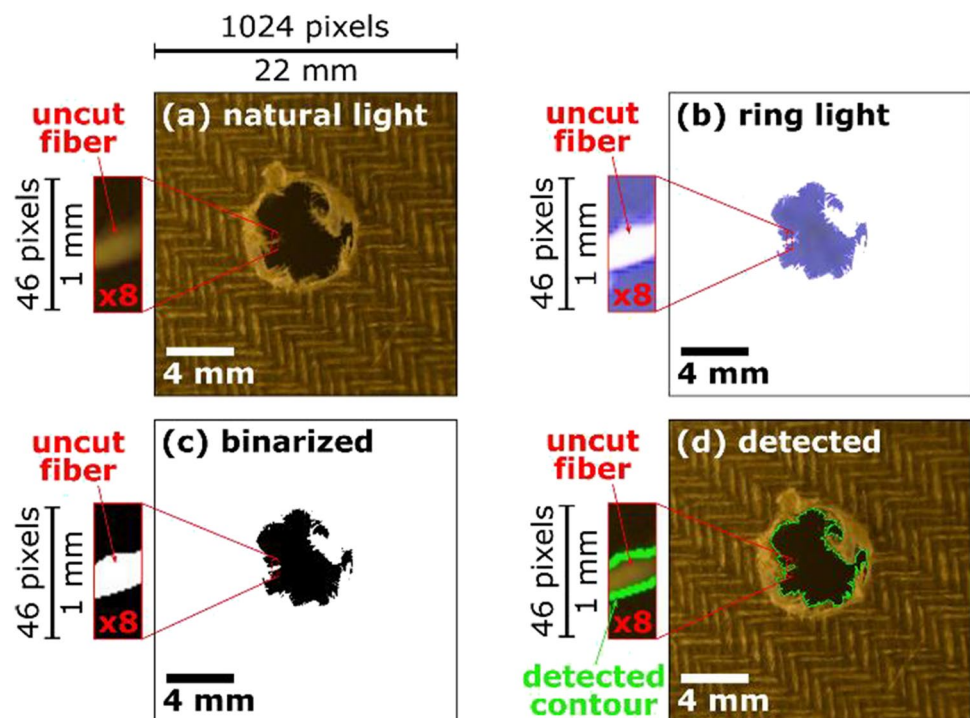
It allowed testing 72 cutting parameters ensuring three holes per parameter. The same drill was used in drilling since preliminary tests showed negligible tool wear after drilling 216 holes using given HSS drill. Selected cutting speed (v_c) ranged from 5 to 200 m/min and feed per tooth (f_z) from 50 to 100 $\mu\text{m}/\text{tooth}$ —see Fig. 6.

3.2 Hole measurements

Custom-built Python scripts controlled the developed measurement station. The robot follows the predefined pattern of the drilled holes, automatically changing the light intensity, capturing drilled holes, and storing images in a respective database catalog while hyperlinked to each of the used cutting data. In parallel, the developed Image Processing scripts analyze the images detecting contours and quantifying them.

The Image Processing of the captured holes (Fig. 5a) was done in Python using OpenCV library (opencv.org). The algorithm for uncut fiber detection consists of intensifying the ring light (Fig. 5b), binarizing the captured image (Fig. 5c), and tracing black/white pixels to detect the interested contour (Fig. 5d).

Fig. 5 Image processing algorithm to detect the contour of uncut fibers. The algorithm consists of **a** capturing the image with natural light to see all defects, **b** intensifying ring light to enhance the contrast, **c** binarizing the enhanced image to define the boundary of uncut fibers, and **d** pixel tracking to define the defect contour. The demonstrated hole in Flax/PLA biocomposite was drilled using new 6.5-mm HSS drill with cutting speed (v_c) of 20 m/min and feed (f_z) of 50 $\mu\text{m}/\text{tooth}$. The area of detected uncut fibers is 12.2 mm^2



The crucial step is the intensification of the light using LED ring to enhance the contrast between uncut fibers and the background. It simplifies the Image Processing making binarization the only procedure needed. Binarization archives splitting all image pixels to two classes (biocomposite and background) without additional filtering. The same procedure can be done using k-mean clustering but takes longer time.

Method precision is determined using Intersection over Union (IoU) metric. The reference value of IoU was measured manually for selected holes. Finally, IoU was from 0.96 to 0.99 with average of 0.97.

The detected contour of uncut fibers describes inner line of defects. The area of uncut fibers is selected quality metric to quantify the defect size. To calculate the area of uncut fibers using detected contour, the area of defined contour was subtracted from the hole area (which is 33.2 mm², according to drill diameter 6.5 mm).

4 Results and discussions

The current section presents the benchmarking of the biocomposite machinability using HSS drills and selected cutting data, tool life tests of the most efficient cutting data, and tool wear analysis.

4.1 Benchmarking

The results of the benchmarking are presented in Fig. 6. Bubble plot shows the area of uncut fibers as the result of Flax/PLA biocomposite drilling using the cutting data in the selected range. The bubble size corresponds to the uncut fiber area from 0 to 15 mm².

The drilling with cutting speed below 60 m/min is accompanied with formation of large defects from 10 to 15 mm². The lowest area of uncut fibers—below 1 mm²—was observed for cutting speed of $v_c = 80$ m/min and feeds $f_z = 50$ μm/tooth and $f_z = 60$ μm/tooth.

The drilling process for the benchmarking on CNC milling machine with developed vacuum table takes ca. 15 min including the movements between holes. The panel measurement using developed measurement system takes approx. 3 min including defect detection, quantification, and results plotting. Totally, the entire benchmarking procedure takes 18 min—or 5 s per hole—if the tool wear check is not carried out. Based on authors’ experience, the same procedure takes at least 3 to 4 h if performed manually. Additionally to the significant time efficiency and minimized labor intensity, the developed method ensures that the analyzed data are insensitive to the human factor.

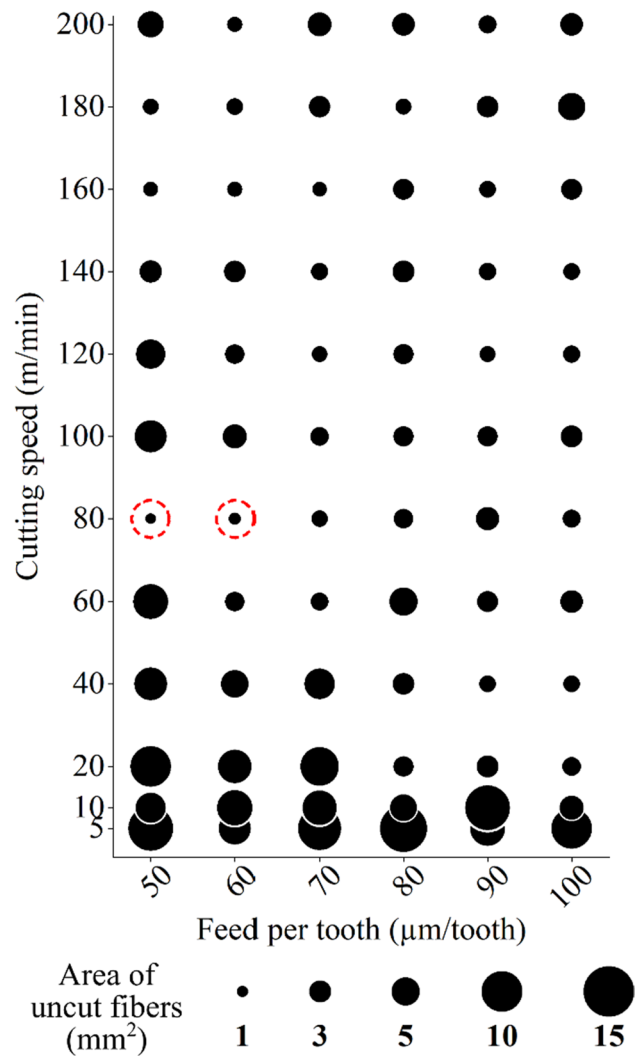


Fig. 6 Machinability benchmarking results of Flax/PLA biocomposite using twist HSS drills. The bubble plot presents the average hole quality for each cutting data point within the considered range of conditions. The hole quality is based on the area of uncut fibers. Each bubble is an average of three measured holes. The error bars are not shown because of the small values (up to 1–3%). Dashed red circles highlight conditions which yield the uncut fiber area below 1 mm²

4.2 Tool life test

The tool flank wear after drilling 216 holes was up to 2 μm, while CER was increased by up to 2 μm. Since the light optical microscope Alicona InfiniteFocus 3D, which was used for wear measurements, has an accuracy of 1 μm, it was decided to accept wear neglectable. Therefore, the following tool life test has been done. The cutting data which provides the best quality and performance (cutting speed 80 m/min and feed 60 μm/tooth) was used.

The behavior of the uncut fiber area over number of drilled holes using new drill is presented in Fig. 7. Uncut

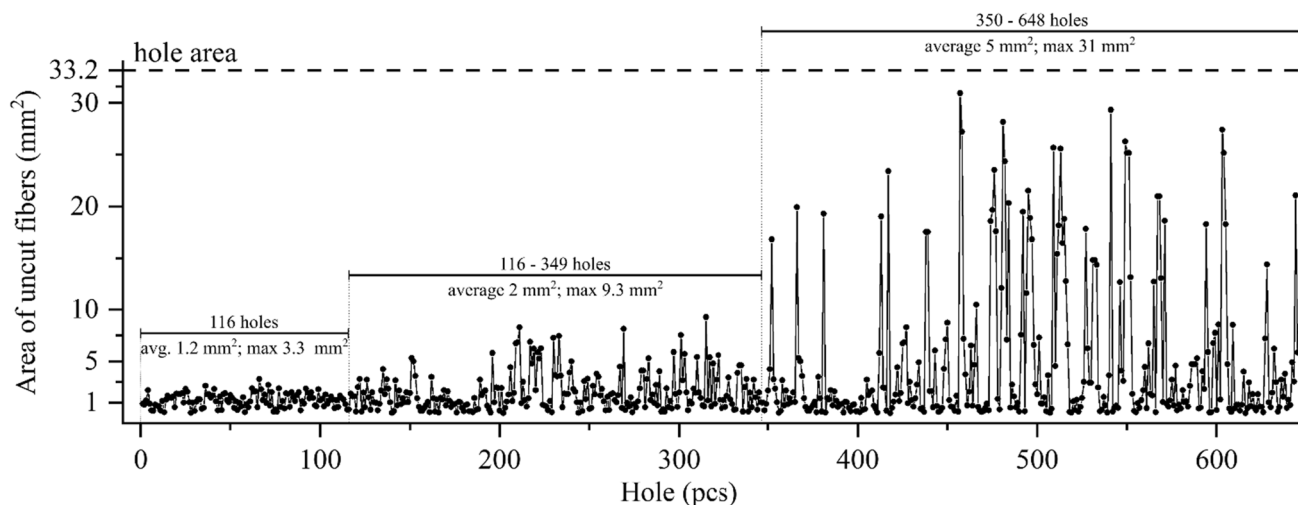


Fig. 7 The behavior of the uncut fiber area over the number of drilled holes as the HSS drill wears down (cutting speed $v_c = 80$ m/min and feed $f_z = 60$ μ m/tooth)

fiber area varies from 0.01 to 3.3 mm² with an average of 1.2 mm² for the first 116 holes when the tool wear was not detectable. The increase of the cutting edge radius from initial 8 to 11 μ m led to increasing of the uncut fiber area to average of 2 mm² and maximum of 9.3 mm². The last 350–648 holes had a much more significant uncut fiber area averaging to 5 mm² and having a maximum of 31 mm² covering almost the entire drilled hole.

The cutting edge radius increased up to $CER = 52$ μ m on the periphery of the cutting edge but remained 11–15 μ m along the rest of the edge. To investigate the micro changes of the tool wear, the cross section of the cutting edges has been done. SEM images of the peripheral regions of new and worn drills are shown in Fig. 8.

The cross section of new drills in regions *i* and *ii* (see Fig. 8) shows the initial burr on the cutting edge. It is the defect after the grinding of the flank face. The cross section of the worn drill in the same regions *i* and *ii* shows that cutting edge is deformed. The cutting edge deforms towards the rake face of the drill, thus creating the negative rake angle. Additionally, the deformed part creates the flank wear of $VB = 105$ μ m in the periphery increasing the contact between flank and machined surface of biocomposite. Altogether, both features are a source of the dramatical increase of the uncut fiber area.

4.3 Measurement system

As with all measuring systems, the accuracy and reliability of any system are of vital importance. As previously described, the imaging system has been constructed in such a way as to yield comparable results

to measurements made in a light-optical microscope. Arguably, an even higher resolution camera and higher magnification could pick up even more detail but at the expense of an increased need for data processing and thus processing time. Thus, in the authors mind, the developed solution has an adequate accuracy for majoring of FRP drilling situations and cases, although, depending on scenario, additional in-depth analysis of particularly interesting hole features may on some occasions require further analysis of the defect formation with higher resolution optics.

The described method of using a vacuum table during the drilling operation, further accompanied by an automated measuring station centered around image acquisition and analysis, has a large potential to drastically streamline the process of experimentally analyzing drilled holes in FRP. As indicated by the demonstration, the solution can decrease the time required for this process 5–6 times compared to manual inspection. Thus, the method enables for a much larger dataset when evaluating defect formation in the drilling FRP or other fiber-reinforced composites.

Given the increased speed of data collection and analysis, it is plausible that the novel methodology presented in this paper will result in a rise of new knowledge on the tool wear and hole defects in drilling of FRP. By using the developed method, it will be possible to analyze the progression of tool wear and related material and hole defects, an analysis which previously has been practically impossible at least on a large scale. Since the following influx of large new datasets generated by the method including images of thousands of drilled holes, this would further require new solutions for efficient hole quality assessment.

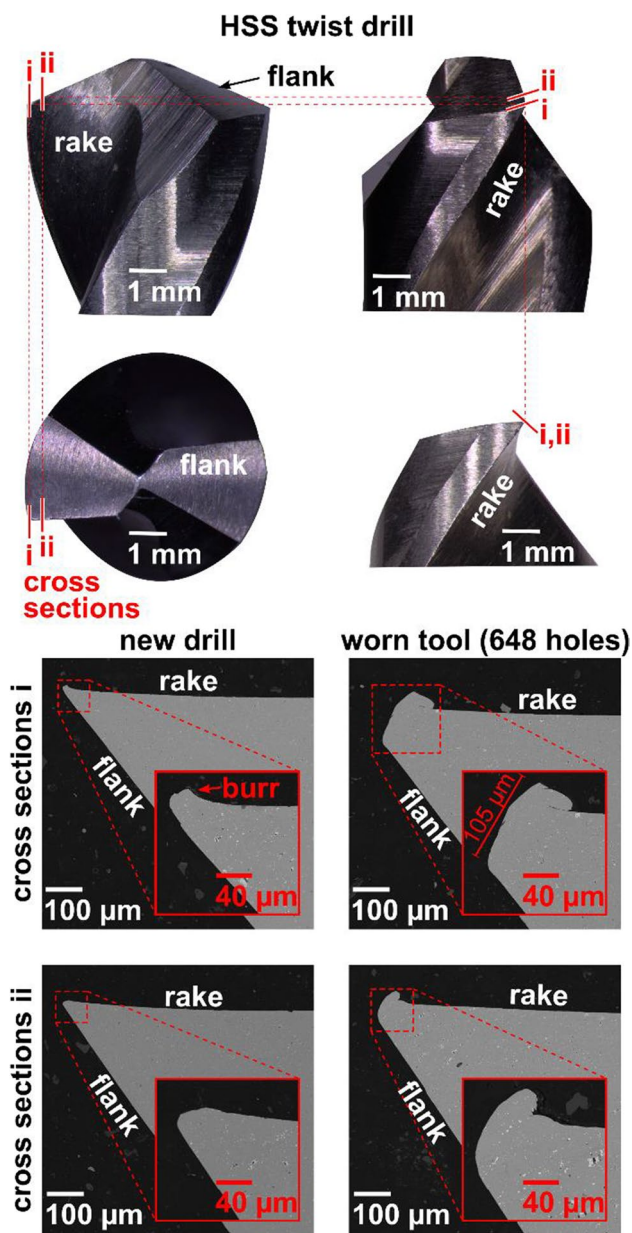


Fig. 8 New and worn HSS drills. SEM images of the cross sections of cutting edges showing the deformation of the cutting edge for the worn tools which leads to creation of the negative clearance angle and increases the contact on the flank

5 Conclusions

This paper describes a developed research solution for studying the drilling of fiber-reinforced polymers. The solution consists of the developed vacuum table, robot arm with high-speed camera, developed top and bottom lighting systems, and image processing algorithms for defect detection from captured images. The novelty of the developed solution corresponds to the combination of the drilling setup, measurement station, and decision-making system which work seamlessly to provide

fast and accurate research process. The results show that the system reaches 5 s per hole including drilling and full cycle of measurements having measurement error of 1–3%.

The system is tested on benchmarking and tool life test when drilling Flax/PLA biocomposite using HSS twist drills. The results show how the developed solution can be used for high routine research activities. The output data, including tested 72 cutting data parameters and full-size tool life test, allowed identifying the operational window for HSS drills and the range of tool life, where drill ensures a certain hole quality.

Acknowledgements The authors thank Mr. Ryszard Wierzbicki from Lund University (Sweden), for the help in manufacturing the vacuum table and drilling of biocomposites. The authors thank Mr. Anirudh Kashyap Hindupur for the help in drilling of biocomposites. The authors thank Dr. Volodymyr Bushlya from Lund University (Sweden), for the help in sample preparation, SEM of drills, and paper reviewing. The authors acknowledge OptiPCDrill project (2021-02139) funded by Vinnova Sweden's Innovation Agency and Zentrales Innovations program Mittelstand (ZIM). The authors thank the sustainable production initiative (SPI), a cooperation between Lund University and Chalmers University of Technology.

Funding Open access funding provided by Lund University.

Declarations

Ethics approval Not applicable

Consent to participate All authors agree to participate.

Conflict of interest The authors declare no competing interests.

Open Access This article is licensed under a Creative Commons Attribution 4.0 International License, which permits use, sharing, adaptation, distribution and reproduction in any medium or format, as long as you give appropriate credit to the original author(s) and the source, provide a link to the Creative Commons licence, and indicate if changes were made. The images or other third party material in this article are included in the article's Creative Commons licence, unless indicated otherwise in a credit line to the material. If material is not included in the article's Creative Commons licence and your intended use is not permitted by statutory regulation or exceeds the permitted use, you will need to obtain permission directly from the copyright holder. To view a copy of this licence, visit <http://creativecommons.org/licenses/by/4.0/>.

References

- Ko FK, Wan LY (2016) Textile structural composites: from 3-D to 1-D fiber architecture. In: The structural integrity of carbon fiber composites: fifty years of progress and achievement of the science, development, and applications, pp 795–847. https://doi.org/10.1007/978-3-319-46120-5_27/FIGURES/40
- Che D, Saxena I, Han P, Guo P, Ehmann KF (2014) Machining of carbon fiber reinforced plastics/polymers: a literature review. *J Manuf Sci Eng*:136. <https://doi.org/10.1115/1.4026526/376924>
- Khashaba UA (2022) A novel approach for characterization of delamination and burr areas in drilling FRP composites. *Compos Struct* 290:115534. <https://doi.org/10.1016/J.COMPSTRUCT.2022.115534>

4. Abrão AM, Faria PE, Rubio JCC, Reis P, Davim JP (2007) Drilling of fiber reinforced plastics: a review. *J Mater Process Technol* 186:1–7. <https://doi.org/10.1016/J.JMATPROTEC.2006.11.146>
5. Teti R (2002) Machining of composite materials. *CIRP Annals* 51:611–634. [https://doi.org/10.1016/S0007-8506\(07\)61703-X](https://doi.org/10.1016/S0007-8506(07)61703-X)
6. Chen WC (1997) Some experimental investigations in the drilling of carbon fiber-reinforced plastic (CFRP) composite laminates. *Int J Mach Tools Manuf* 37:1097–1108. [https://doi.org/10.1016/S0890-6955\(96\)00095-8](https://doi.org/10.1016/S0890-6955(96)00095-8)
7. Capello E, Langella A, Nele L, Paoletti A, Santo L, Tagliaferri V (2008) Drilling polymeric matrix composites. In: *Machining: fundamentals and recent advances*, pp 167–194. https://doi.org/10.1007/978-1-84800-213-5_6/COVER/
8. Wang C, Cheng K, Rakowski R, Greenwood D, Wale J (2017) Comparative studies on the effect of pilot drillings with application to high-speed drilling of carbon fibre reinforced plastic (CFRP) composites. *Int J Adv Manuf Technol* 89:3243–3255. <https://doi.org/10.1007/S00170-016-9268-Y/METRICS>
9. Cao S, Li HN, Tan G, Wu C, Huang W, Zhou Q et al (2023) Bi-directional drilling of CFRPs: from principle to delamination suppression. *Compos B Eng* 248:110385. <https://doi.org/10.1016/J.COMPOSITESB.2022.110385>
10. Voß R, Henerichs M, Rupp S, Kuster F, Wegener K (2016) Evaluation of bore exit quality for fibre reinforced plastics including delamination and uncut fibres. *CIRP J Manuf Sci Technol* 12:56–66. <https://doi.org/10.1016/J.CIRPJ.2015.09.003>
11. de Albuquerque VHC, Tavares JMRS, Durão LMP (2009) Evaluation of delamination damage on composite plates using an artificial neural network for the radiographic image analysis: <http://DxDoiOrg/101177/0021998309351244>. 44:1139–1159. <https://doi.org/10.1177/0021998309351244>
12. Zhang H, Zhu P, Liu Z, Qi S, Zhu Y (2020) Research on prediction method of mechanical properties of open-hole laminated plain woven CFRP composites considering drilling-induced delamination damage. <https://DoiOrg/101080/1537649420201745969>. 28:2515–2530. <https://doi.org/10.1080/15376494.2020.1745969>
13. Giasin K, Ayvar-Soberanis S (2017) An investigation of burrs, chip formation, hole size, circularity and delamination during drilling operation of GLARE using ANOVA. *Compos Struct* 159:745–760. <https://doi.org/10.1016/J.COMPSTRUCT.2016.10.015>
14. Romoli L, Lutey AHA (2019) Quality monitoring and control for drilling of CFRP laminates. *J Manuf Process* 40:16–26. <https://doi.org/10.1016/J.JMAPRO.2019.02.028>
15. Xu J, el Mansori M (2016) Experimental study on drilling mechanisms and strategies of hybrid CFRP/Ti stacks. *Compos Struct* 157:461–482. <https://doi.org/10.1016/J.COMPSTRUCT.2016.07.025>
16. John KM, Thirumalai KS (2020) Backup support technique towards damage-free drilling of composite materials: a review. *Int J Lightweight Mater Manuf* 3:357–364. <https://doi.org/10.1016/J.IJLMM.2020.06.001>
17. Xu C, Yao S, Wang G, Wang Y, Xu J (2021) A prediction model of drilling force in CFRP internal chip removal hole drilling based on support vector regression. *Int J Adv Manuf Technol* 117:1505–1516. <https://doi.org/10.1007/S00170-021-07766-0/FIGURES/13>
18. Wang M, Xu C, Zou A, Wang G, Wang Y, Yao S et al (2022) Design of internal flow passage of internal chip removal drill for suction-type internal chip removal system. *Int J Adv Manuf Technol* 119:4191–4202. <https://doi.org/10.1007/S00170-021-08430-3/FIGURES/16>
19. Maghami A, Salehi M, Khoshdarregi M (2021) Automated vision-based inspection of drilled CFRP composites using multi-light imaging and deep learning. *CIRP J Manuf Sci Technol* 35:441–453. <https://doi.org/10.1016/j.cirpj.2021.07.015>
20. Faraz A, Biermann D, Weinert K (2009) Cutting edge rounding: an innovative tool wear criterion in drilling CFRP composite laminates. *Int J Mach Tools Manuf* 49:1185–1196. <https://doi.org/10.1016/J.IJMACHTOOLS.2009.08.002>
21. Hrechuk A, Bushlya V, Ståhl JE (2018) Hole-quality evaluation in drilling fiber-reinforced composites. *Compos Struct* 204:378–387. <https://doi.org/10.1016/J.COMPSTRUCT.2018.07.105>
22. Hrechuk A, Bushlya V, Ståhl JE, Kryzhanivskyy V (2021) Novel metric “Implenarity” for characterization of shape and defectiveness: the case of CFRP hole quality. *Compos Struct* 265:113722. <https://doi.org/10.1016/J.COMPSTRUCT.2021.113722>
23. Hrechuk A (2023) Recognition of drilling-induced defects in fiber reinforced polymers using machine learning. *Procedia CIRP* 117:384–389. <https://doi.org/10.1016/J.PROCIR.2023.03.065>
24. Hindupur AK (2022) Effect of cutting parameters on hole defects while drilling twill reinforced bio-composites. Lund University, Master Thesis LUTMDN/(TMMV-5338)/1-97/2022. <https://lup.lub.lu.se/student-papers/record/9088480>. Accessed May 2023

Publisher's note Springer Nature remains neutral with regard to jurisdictional claims in published maps and institutional affiliations.